SURFACE MOBILITY THROUGH ACOUSTOELECTRIC INTERACTION

BY

John Herbert Cafarella

SUBMITTED IN PARTIAL FULFILLMENT

OF THE REQUIREMENTS FOR THE DEGREE OF

MASTER OF SCIENCE IN ELECTRICAL ENGINEERING

at the

MASSACHUSETTS INSTITUTE OF TECHNOLOGY

January, 1973

Signature Redacted

Signature of Author _____

Department of Electrical Engineering, January 24, 1973

Signature Redacted

Certified by _____

Thesis Supervisor

Signature Redacted

Accepted by _____

Chairman, Departmental Committee on Graduate Students

SURFACE MOBILITY THROUGH ACOUSTOELECTRIC INTERACTION

BY

John Herbert Cafarella

Submitted to the Department of Electrical Engineering on January 24, 1973 in partial fulfillment of the requirements for the Degree of Master of Science in Electrical Engineering

ABSTRACT

The sheet mobility of electrons in an accumulation layer on silicon has been determined by measuring the acoustoelectric current which accompanies the interaction between the electrons and piezoelectric surface waves on $LiNbO_3$. Since carrier densities are controllable with a normal electric field, either minority or majority carrier mobilities may be explored. By using sufficiently high-frequency ultrasound, the effects of surface states on the mobility measurement can be made negligible. For these two reasons such a surface mobility measurement has distinct advantages over the usual field-effect method. Most important, however, is that this measurement is direct, not needing the carrier density to find the mobility. We have carried out measurements for the mobility of electrons accumulated on high-resistivity (30,000 Ω-cm) silicon. Acoustic surface waves at 166 MHz were used to induce the accumulated electron density from $1.5 \times 10^{10}/cm^2$ to $5 \times 10^{11}/cm^2$. Over this range the surface mobility varies, respectively, from 1100 to 450 cm^2/volt-sec.

THESIS SUPERVISOR: Abraham Bers

TITLE: Professor of Electrical Engineering

TABLE OF CONTENTS

INTRODUCTION 5

1 THEORY

1.A Acoustoelectric Current Phenomenon 6

1.A.1 Acoustoelectric amplification 6
1.A.2 The acoustoelectric current 6

1.B Trapping Effects 8

1.B.1 Trapping mechanism 8
1.B.2 Trapping factor 9
1.B.3 Acoustoelectric current with trapping 10

2 EXPERIMENT

2.A Theory of Experiment 12

2.A.1 General experiment 12
2.A.2 The experiment performed 12

2.B Parameter Evaluation 13

2.B.1 Acoustic wave velocity 13
2.B.2 Interaction length 13
2.B.3 Power dissipated 13
2.B.4 Current 14

2.C Test Fixture 14

2.C.1 Configuration 14
2.C.2 Assembly 15

2.D Silicon Processing 15

2.D.1 Chemical processing 15
2.D.2 Cleaning and oxide thinning 16
2.D.3 Uniformity probe 16
2.D.4 Monitor M.O.S. conductance 17

2.E Delay-Line Processing 17

2.E.1 Substrate 17
2.E.2 Transducers 17
2.E.3 Rails 18
2.E.4 Charging 18

2.F Pre-experiment Tests 18

2.F.1 Linearity with power 18
2.F.2 Mechanical contact 19
2.F.3 Sheet model 19

3 RESULTS

3.A Data 21

3.B Mobilities 21

3.C Consistency 22

APPENDICES

A Acoustoelectric Current 24

B Trapping Factor 32

C Sheet Model 36

D Calculations 41

NOTES 45

FIGURES 47

ACKNOWLEDGMENTS 56

INTRODUCTION

We have used the acoustoelectric current to measure electron mobilities at silicon surfaces. This method has several advantages over other mobility measurements. The carrier density being controllable with a transverse electric field, this method may be used to measure both majority and minority carriers on the same sample. Surface states, whose effects interfere with other mobility measurement methods, have no effect at high frequencies. Since ultrasonic frequencies may be large, trapping effects due to surface states may be avoided with this method. The most significant difference between this and other methods, however, is that this is a direct mobility measurement, which does not require a density determination to yield the mobility. Only directly measurable quantities are involved in determining the mobility. The particular experiment performed, in order to demonstrate the reliability of this new method, used very low surface state density silicon samples and only explored electron mobilities.

1. THEORY

1.A ACOUSTOELECTRIC CURRENT PHENOMENON

1.A.1 Acoustoelectric Amplification

Bulk acoustic-wave amplifiers were the subject of investigation in the early sixties. The gain mechanism, analogous to that of a travelling-wave tube, involved interaction between drifting electrons and bulk acoustic waves in a piezoelectric semiconductor.[1] With the advent of surface-wave technology, work was begun on surface-wave amplifiers.[2] One of the outstanding features of the surface interaction is that the drifting electrons may be located in an adjacent medium rather than within the acoustic medium. This allows for independent optimization of semiconductor and piezoelectric properties. A recent amplifier effort at Lincoln Laboratory involved surface waves on $LiNbO_3$, interacting with electrons in an accumulation layer on an adjacent piece of silicon.[3]

1.A.2 The Acoustoelectric Current

When drifting electrons interact with acoustic waves, there is a change in the D.C. current in the silicon, analogous to the shift in operating point of a transistor amplifier under signal.[4] Consider the accumulation-layer amplifier structure. (See Fig. 1.)

We model the silicon as a sheet conductance, that of the accumulation layer. Bulk conduction is neglected. This model will be valid only if the accumulation-layer density is much larger than the bulk and the accumulation-layer thickness is small compared to the acoustic wavelength. (See Appendix C.) The sheet current density is

$$J_s = e\mu n_s E + eD \frac{\partial n_s}{\partial z},$$

where e = electron charge magnitude; μ = electron mobility; n_s = electron sheet density; E = electric field; and D = diffusion coefficient.

If n_s and E are assumed to have a constant term and a small-signal A.C. component, we have

$$J_s = e\mu n_{s0}E_0 + e\mu(n_{s0}E_1 + n_{s1}E_0) + e\mu n_{s1}E_1 + eD\frac{\partial n_{s1}}{\partial z}.$$

In the linear analysis of the amplifier, the second-order term, $e\mu n_{s1}E_1$, is dropped and the current equation becomes

$$J_{s1} = e\mu(n_{s0}E_1 + n_{s1}E_0) + eD\frac{\partial n_{s1}}{\partial z}.$$

In finding the change in D.C. current due to the presence of an acoustic wave, however, it is precisely this second-order term we seek. Since the first-order quantities are sinusoidal, only a product of them will have a D.C. effect. The acoustoelectric current density is

$$\begin{aligned} J_{AE} &= \langle J_s \rangle - J_0 \\ &= e\mu \left\langle n_{s0}E_1 + n_{s1}E_0 + n_s E_1 \right\rangle + eD\left\langle \frac{\partial n_{s1}}{\partial z} \right\rangle \end{aligned}$$

or

$$J_{AE} = e\mu \langle n_{s1}E_1 \rangle .$$

As shown in Appendix A, the linear analysis may be used to express the current density as

$$J_{AE} = \frac{\mu}{v_s} 2k_i P_A,$$

where k_i = imaginary part of wave number, and P_A = acoustic sheet power.

When this current density is related to the shift in terminal current, we find

$$I_{AE} = \frac{\mu}{v_s}\frac{P_D}{L},$$

where I_{AE} = acoustoelectric current; μ = mobility; v_s = sound velocity; P_D = power given to the silicon by the acoustic wave (not constrained to be positive), and L = interaction length.

Since an interaction exists even in the absence of a drift field, this acoustoelectric current will be the short-circuit current measured at the silicon terminals when an acoustic wave passes by.

1.B TRAPPING EFFECTS

1.B.1 Trapping Mechanism

The effect of "traps" on bulk semiconductor properties has been extensively studied.[5] Similar studies exist for "surface states" at semiconductor surfaces.[6] While arising from different sources, these two phenomena have the same effect on the A.C. behavior of a device. Since we are interested in semiconductor surfaces, surface states are of main concern. It may be noted that while trapping effects in bulk acoustic interaction have been studied,[7] they are relatively unexplored in surface interaction.

A surface state is localized to the semiconductor surface,[8] unlike a Bloch state which propagates through the bulk. This is similar to the localization effect of bulk traps. However, while bulk traps are primarily ionized donors or acceptors, surface states are not nearly so easily explained or analyzed. Surface states arise from the disruption of the periodic crystal potential at the surface. Although there have been attempts at analytic solutions for surface states, results are limited. The density of surface states has experimentally been found to depend on crystal orientation and surface preparation. While freshly cleaved surfaces in vacuum have surface-state densities approaching the surface density of atoms, properly passivated surfaces can have densities which are entirely negligible. The latter is thought to be due to the "less abrupt" termination of the lattice potential.

The D.C. effect of traps is obvious, but it is the A.C. behavior which makes trapping worth investigating. Given an equilibrium carrier density, we superimpose a small-signal bunched density. Since the quasi-Fermi level is fluctuating with the bunched density, the surface states around the Fermi level are filling and emptying at the signal frequency. This means that only a fraction of the small-signal bunched carrier density will be mobile, the rest being trapped in surface states.

1.B.2 Trapping Factor

To allow solution of the dynamical equations in the presence of surface states, a "trapping factor," $f(\omega)$, has been defined, similar to the bulk. It is the ratio of mobile bunched carrier density to the total. In the linearized A.C. equations, we must multiply the small-signal density in the current equation by the trapping factor, since not all of these carriers will be able to move under the influence of drift and diffusion.

The trapping factor is derived in Appendix B. The ratio of mobile small-signal bunched electron density to the total, f, is best examined by forming

$$\frac{1}{f} - 1 = \left(\frac{1}{f_0} - 1\right)\left[\frac{\ln(1 + j\omega\bar{\tau})}{j\omega\bar{\tau}}\right].$$

This is just the ratio of trapped bunched density to mobile bunched density. From the Appendix we see the following:

1) $\bar{\tau} = \frac{1}{n_{s0} C}$, where n_{s0} = equilibrium sheet electron density and C = capture probability for an electron, is a time constant which is characteristic of the traps (at density n_{s0}).

2) For $\omega\tau \ll 1$ we have

$$\frac{1}{f} - 1 \simeq \frac{1}{f_0} - 1 \quad \text{or} \quad f \simeq f_0.$$

This low-frequency asymptote represents the situation when the traps are able to equilibrate with the electrons. Since

$$\frac{1}{f_0} - 1 = \frac{kTN_{ss}(E_F)}{n_{s0}},$$

f_0 is determined by the ratio of accessible traps (within kT of the Fermi level) to the sheet electron density.

3) For $\omega\tau \gg 1$ we have

$$\frac{1}{f} - 1 \approx 0 \quad \text{or} \quad f \approx 1.$$

This says that, at high frequencies, trapping effects are negligible. This is reasonable because at high frequencies the traps not only cannot equilibrate with the electrons, but the fluctuations are so rapid that the traps cannot respond at all.

1.B.3 Acoustoelectric Current with Trapping

The dependence of the acoustoelectric current, with traps present, is derived in Appendix A.

$$I_{AE} = \frac{\mu}{v_0} \frac{P_d}{L} \operatorname{Re}\left\{ f(\omega) \right\},$$

where μ = the effective sheet mobility; v_s = acoustic wave velocity; P_d = the power given up by the acoustic wave to the silicon; L = the interaction length, and $f(\omega)$ = the trapping factor of Appendix B, which accounts for some of the electrons being bound in surface states. $\operatorname{Re}\left\{f(\omega)\right\}$ is shown in Fig. 2.

We see that the current will be, at low frequency, some fraction of the high-frequency value, where traps have no effect. Since all other parameters are otherwise determinable, an acoustoelectric current measurement yields the mobility. Other surface-mobility measurement techniques are constrained to relatively low frequencies, and are, hence, confused by the presence of surface states. Leistiko et al.[9] have used field-effect conductivity measurements coupled with M.O.S. conductance measurements to evaluate the surface mobility in the presence of surface states. Acoustic-wave frequencies may be rather large, so acoustoelectric current measurements represent a simplified technique of evaluating mobility for samples with traps, by using a frequency at which the traps do not respond.

2. EXPERIMENT

2.A THEORY OF EXPERIMENT

2.A.1 General Experiment

We are interested in measuring the carrier surface mobility as a function of band-bending. Various levels of band-bending are attainable by applying an electric field normal to the silicon surface; the method will be described later. Ideally, a value of bias (band-bending) would be selected, and the quantities P_d, v_s, and L determined as the frequency is varied. This allows $\mu Re(f(\omega))$ to be calculated, and the high-frequency asymptote is simply the mobility corresponding to the value of band-bending. Actually, it is much easier to vary the bias than the frequency, so the experiment is best performed at a number of frequencies, each time varying the bias over the desired range. Overlays of the various mobility-vs.-band-bending curves should yield a unique maximum mobility-vs.-band-bending. This is the actual surface mobility.

2.A.2 The Experiment Performed

There are a number of things which might interfere with the ideal operation of the acoustoelectric-current mobility measurement. For this reason, a limited experiment has been undertaken to demonstrate the feasibility of this new method. The following limitations were imposed on the experiment:

a) We measure only the electron mobility in an accumulation layer on N-type silicon. In the more general experiment, minority- and majority-carrier mobilities may be explored since the band-bending is controllable.

b) Since this new method of mobility measurement claims to avoid confusion due to surface states, we must show that it gives correct results when there are no traps present. The silicon sample used in the experiment was prepared, as will be described, so as to have negligible surface-state densities.

2.B PARAMETER EVALUATION

2.B.1 Acoustic-wave Velocity

The Rayleigh wave velocity for various cuts and directions have been published, and have been checked by members of Group 86, Lincoln Laboratory, to be 3485 m/sec for Y-cut, Z-propagating $LiNbO_3$.

2.B.2 Interaction Length

The interaction length is the length of the accumulation layer on the silicon. The contacts are not included because the N^+ regions have negligible acoustoelectric interaction. Accumulated area on the silicon surface is determined by a protective mask on the SiO_2 before its removal for the N^+ diffusion. The length of this area was taped to be 400 mm, and checked after processing with a crossed-hair microscope.

2.B.3 Power Dissipated

The acoustic power incident to the active area is the power into the line less the input-transducer loss. A standard power meter was used to measure the power into the line. The delay line was stub-tuned, so that power reflection was negligible. The effect of diffraction is excess loss at the output transducer, and the transducers are assumed identical. Therefore, the input-transducer loss is taken to be half the difference between the delay-line insertion loss and the estimated diffraction losses.[10]

To determine the amount used of the power incident to the active area, the difference between the overall insertion loss and the delay-line loss must be measured. This excess insertion loss is due to the interaction.

2.B.4 Current

The acoustoelectric current was determined by measuring the voltage and sample resistance on a Kiethly electrometer. This was done for two reasons:

1) In measuring very low currents, ammeter resistances tend to be large compared to a megohm. Since the samples used had resistances in the order of a megohm, it would be very hard to find an ammeter which is a "short." However, a Kiethly electrometer used as a voltmeter is an excellent "open" at 10^{14} Ω.
2) The second reason for not measuring current is that the effects of semiconductor contacts become a problem. If, instead, the open-circuit voltage is measured, there are no contact problems.

2.C TEST FIXTURE

2.C.1 Configuration

In Fig. 3 there appears a diagram of the mechanical assembly used in the acoustoelectric-current experiment. This is identically the structure used in accumulation-layer amplifier work. Resting on the Plexiglas base is a piece of "Neesi" glass. This has its upper surface coated with tin oxide to form the field plate of the structure. A $LiNbO_3$ delay line is thermally bonded to the Neesi glass, and the Si sample rests on the delay-line rails. A clamp arrangement (not shown) allows for ad-

justment of the gap between the silicon and the $LiNbO_3$, and also electrical contacts to the silicon.

2.C.2 Assembly

The delay line is bonded to the glass with crystal mounting wax. A very thin layer of wax is used, and light interference fringes are observed while moving the delay line so that the variation in the gap between glass and $LiNbO_3$ is minimized. This is to prevent distortion of the electrostatic field between the field plate and the silicon. The silicon sample is placed, accumulated side down, on the SiO_2 rails of the delay line, centered on the acoustic-wave channel. The bottom piece of the clamp is positioned over the silicon and contact electrodes are inserted. The top clamp piece is also slid over the guide screws, contacts are aligned, and locking nuts tightened down. Six set screws, which apply pressure between the upper and lower clamp pieces, are then manipulated while the operator observes, through the bottom, the interference fringes between the Si and the $LiNbO_3$. In this way a uniform gap is obtained over the acoustic channel.

2.D SILICON PROCESSING

2.D.1 Chemical Processing

High-resistivity (30,000 Ω-cm) silicon is purchased. The low doping level ($N_A - N_D = n_0 \approx 10^{11}$ cm^{-3}) is achieved by compensation techniques. A phosphorus diffusion at the ends of the silicon wafer provides N^+ regions for good electrical contact between the silicon and the gold contacts which are sputtered on. The protective oxide, used in the N^+ diffusion, is removed from the backside of the wafer. The oxide on the

front side is left on, thus maintaining an accumulation layer (due to oxide charge) at zero bias.

Low surface-state density is assured by the orientation and oxide preparation. The surface normal (100) is known to be a minimum of the surface state vs. orientation. The oxide was grown in dry O_2 and annealed in N_2. Phosphorous glass, formed on the oxide during N^+ diffusion, was used as a getter for impurities.

2.D.2 Cleaning and Oxide Thinning

Cleaning a silicon sample is achieved by boiling (in order) in J-100 cleaner, trichlor, ethanol, and distilled, de-ionized (D-I) water. Samples are diced from the processed wafer. When they are first obtained, the oxide ($\approx$1200 Å) contains so much charge that the Si surface is strongly accumulated. In order to reduce this zero-bias accumulation, and also to lessen the ultimate gap between the silicon and $LiNbO_3$, the oxide is thinned (to $\approx$450 Å) in buffered HF. After thinning the sample is boiled in D-I water to remove any soluble ions. After this, the sample is left for 24 hours while the back of the sample grows a thin, neutral oxide ($\approx$100 Å) by free-air oxidation.

2.D.3 Uniformity Probe

It has been shown that nonuniformities in the accumulation-layer density can have drastic effects on the acoustoelectric interaction. Indeed, this is precisely what limits the low-density acoustoelectric mobility measurement. If a current is applied to a silicon sample, and the voltage probed as a function of length, the numerical derivative of this data yields the conductivity as a function of length.

The graph of Fig. 4 shows that the nonuniformities which limit the low-density mobility measurement are suppressed by applying a transverse field in the experiment.

2.D.4 Monitoring M.O.S. Conductance

The M.O.S. conductance technique has proved[11] to be a reliable source of surface-state density determination. Since surface-state densities depend almost totally upon the oxide preparation, a 1Ω-cm substrate is processed along with the 30,000Ω-cm substrates so that M.O.S. monitor tests may be performed. It is assumed that the 1 Ω-cm monitor substrate has the same surface-state densities as the 30,000 Ω-cm substrates. High surface-state densities show up as a large conductive component in parallel with the M.O.S. capacitance of a gold dot on the silicon surface. To show that the processing techniques are able to control surface-state densities, we show in Fig. 5 the M.O.S. curves for the monitor for BB49 (used in the mobility experiments) which we require to have very low trap density, and another monitor which was prepared to have higher trap densities.

2.E DELAY-LINE PROCESSING

2.E.1 Substrate

The delay line used was a Y-cut $LiNbO_3$ with propagation in the Z-direction. Its thickness was 100 mils, which was thicker than desired but the 28-mil crystals which were available could not be used due to the charging effect to be described later.

2.E.2 Transducers

Interdigital transducers were sputter-deposited on the $LiNbO_3$ substrate.

They were Cr-Au, each having ten finger pairs. Since bandwidth was not a problem, it was feasible to use this large number of fingers, and thus reduce transduction problems. 166 MHz was the center frequency.

2.E.3 Rails

Rails are needed to keep the silicon from loading the surface wave mechanically. Several types of rail material have been tried, but only SiO_2 has proved to be durable and consistent enough to be of use. SiO_2 was sputter-deposited on the delay line 450 Å thick, with a 25-mil channel for the surface wave.

2.E.4 Charging

There is a drift phenomenon which occurs when Si is placed on $LiNbO_3$. It manifests itself in any property involving the silicon, such as resistance or terminal current. The exact nature of the drift is not known, but effects of SiO_2 deposition and $LiNbO_3$ pyroelectricity are currently under investigation. The delay line was chosen to have very low drift. This was done by mounting various delay lines in the test configuration and observing the time stability of the silicon resistance. The drift effect was further reduced by using pulsed bias fields during the experiment.

2.F PRE-EXPERIMENT TESTS

2.F.1 Linearity with Power

As the bunched-carrier density approaches the equilibrium density, we would expect saturation to set in. Therefore, it was necessary to check that, in the acoustoelectric-current measurement, low enough power was

used that the current was linear with power. The graph of Fig. 6 shows that the acoustoelectric current is linear with power well beyond the power range of our experiment.

2.F.2 Mechanical Contact

To check for accidental contact between the silicon and the $LiNbO_3$ in the acoustic channel, two checks were made. First, in assembly, the optical fringes were observed. This always reveals a contact point by its circular pattern and different color. Sometimes, when contact was over a more extensive area, the optical pattern might not catch the fault. A second, electrical, test was performed after the assembly. For very strongly accumulated silicon, the acoustoelectric interaction becomes vanishingly small. Using this fact, it is possible to detect mechanical contact. One need only find the asymptotic loss as the bias voltage becomes large (>1000 V). If this loss approaches the insertion loss of the delay line alone, there could be no excess loss due to mechanical contact.

2.F.3 Sheet Model

It is necessary to check that the sheet model used in analysis is appropriate under the experimental conditions. This becomes difficult for low accumulation density. In the Appendix, sheet density and density distribution are evaluated for surface potentials greater than $\sim 3\,\frac{kT}{e}$. In this region the results may be obtained without numerical integration.

As will be discussed later, nonuniformity in the silicon conductivity limits the range of validity to a surface potential of $\sim 8\,\frac{kT}{e}$. To limit the sheet thickness to about ten times less than the acoustic wave-

length at 166 MHz, it is necessary to have $U_s \geq 8.8\frac{kT}{e}$. This corresponds to an electron sheet density of $n_s \approx 1.5 \times 10^{10}$ cm^{-2}. We see that non-uniformity is the true limiting factor.

3. RESULTS

3.A DATA

Three silicon samples (A, B, C) were scribed from the silicon wafer BB49, 120 mil wide. The active (accumulated) length was 400 mil. Each sample was twice cleaned, mounted, and tested. Of these six runs, representative data from Run #1 on BB49C are presented in Appendix D, along with the associated calculated quantities and the calculations necessary to arrive at the mobility.

3.B MOBILITIES

Mobility measurements were made (at 166 MHz) while the field-plate voltage was varied from a low value (-100 V to 0 V depending on the zero-bias condition of the sample) to 1,000 V. This results in a range of surface densities from 1.5×10^{10} cm^{-2} to 5×10^{11} cm^{-2}, which correspond to surface potentials from $8\frac{kT}{e}$ through $16\frac{kT}{e}$, respectively. In this range the sheet model is easily justified. The lower density limitation is primarily the effect of nonuniformity in the density distribution. The upper limit was due to the limit of 1,000 V (to avoid arcing) and the 100-mil thickness of the delay line. If the 28-mil crystals available had not had the charging problem described, the highest sheet density would have been $\approx 2 \times 10^{12}$ cm^{-2}.

The graph of mobility-vs.-density shows that, for low densities, the mobility approaches the bulk value of 1200 $cm^2/v \cdot sec$, although the scatter due to nonuniformity is obvious at these densities. For higher densities, the nobility is monotonically decreasing, to about

450 $cm^2/v \cdot sec$ at $n_s = 5 \times 10^{11}\ cm^{-2}$.

In Fig. 7 we have a linear graph of mobility vs sheet electron density. Since the sheet density and band-bending are related (see Appendix C), the graph has been relabeled across the top in units of kT/e of band-bending. Thus we have determined mobility vs. band-bending.

3.C CONSISTENCY

As outlined in Appendix D, we may calculate the sheet electron density by two methods. The results of the mobility measurement, coupled with a conductance measurement, yield the sheet density, labeled $n_{s\mu}$. The sheet density may also be calculated from the capacitance of the structure, this labeled n_{sc}. Figure 8 shows $n_{s\mu}$ plotted against n_{sc}. Since these independently determined values are equal within experimental error, this method of measuring mobility appears to be reliable.

Since the effect of traps is to change $n_{s\mu}$ and n_{sc} in opposite directions, the unity slope of Fig. 8 also reassures us that the trap density is negligible.

In Fig. 9 the mobility measured through the acoustoelectric current is compared to theoretical and other experimental mobility values. The shaded area (Curve 1) represents the range of mobilities measured by the acoustoelectric current. The spread due to nonuniformities at low densities is obvious on the semi-logarithmic scale. Although there is significant difference between the measured values and Schrieffer's[12] theory of diffuse scattering (Curve 2), they agree very well with other experimental values. The two experimental methods used conductivity measurements coupled with an alternate experiment to separate the density and

surface-state information. Fowler, Fang, and Hochberg[13] used Hall measurements, while Leistiko, Grove, and Sah[9] used M.O.S. capacitance conductivity measurements.

APPENDIX A

ACOUSTOELECTRIC CURRENT

We start with the current equation, continuity equation, and Gauss' law (for electrons in a sheet):

$$J_s = e\mu n_{sf} E + eD \frac{\partial n_{sf}}{\partial z},$$

$$\frac{\partial J_s}{\partial z} - e \frac{\partial n_s}{\partial t} = 0,$$

$$\frac{\partial E}{\partial z} = - \frac{e}{\epsilon} (n_s - n_{s0}),$$

where J_s = sheet current, E = electric field, μ = effective sheet mobility, e = electron charge magnitude, D = diffusion coefficient, ϵ = dielectric permittivity, n_s = total sheet electron density, n_{s0} = equilibrium sheet electron density, n_{sf} = mobile sheet electron density. (See Figure 1.) The bulk conductivity is negligible compared to the sheet conductivity of the accumulation layer.

J_s, E, and n_s are assumed to have the following components:

$$E = E_0 + E_1,$$

where E_0 = D.C. electric field due to "drift" voltage applied to Si, and E_1 = small-signal A.C. electric field at the accumulation layer due to acoustic wave on $LiNbO_3$;

$$J_s = J_{s0} + J_{s1},$$

where J_{s0} = D.C. sheet current density with no acoustic wave present, and J_{s1} = small-signal A.C. current density due to acoustoelectric interaction; and

$$n_s = n_{s0} + n_{s1} = n_{s0} + n_{s1}^t + n_{s1}^f,$$

where n_{s0} = equilibrium electron sheet density, and n_{s1} = small-signal bunched-electron density which is comprised of n_{s1}^t and n_{s1}^f, the trapped and free bunched densities.

Inserting the assumed forms for J_s, E, and n_s and linearizing for small signals (dropping the $n_{s1}E_1$ term), we have

$$J_{s1} = e\mu(n_{s1}^f E_0 + n_{s0}E_1) + eD\frac{\partial n_{s1}^f}{\partial z},$$

$$\frac{\partial J_1}{\partial z} - e\frac{\partial n_{s1}}{\partial t} = 0,$$

$$\frac{\partial E_1}{\partial z} = -\frac{e}{\epsilon}n_{s1}.$$

Using a travelling-wave dependence ($\exp(j\omega t - jkz)$), and complex amplitudes, and introducing the trapping factor,

$$f \equiv \frac{n_{s1}^f}{n_{s1}}$$

(see Appendix B), we obtain:

$$\begin{aligned} J_{s1} &= e\mu E_0 f\tilde{n}_{s1} + e\mu n_{s0}\tilde{E}_1 - jkeDf\tilde{n}_{s1} \\ &= ev_0 f\tilde{n}_{s1} + \sigma_d\tilde{E}_1 - jkeDf\tilde{n}_{s1}, \end{aligned}$$

$$k\tilde{J}_{s1} = -e\omega\tilde{n}_{s1},$$

$$jk\tilde{E}_1 = \frac{e}{\epsilon}\tilde{n}_{s1},$$

where $v_0 = \mu E_0$ = drift velocity, directed opposite to E_0 for electrons, $\sigma_d = e\mu n_{s0}$ = sheet conductivity; $\sim$ stands for complex amplitude.

These equations lead to the effective conductivity function for the accumulation layer:

$$\tilde{J}_{s1} = \sigma_s(\omega, k)\tilde{E}_1 = \frac{\omega \sigma_d \tilde{E}_1}{\omega - fkv_0 - jfk^2D}.$$

Having solved the linear equations, we may return to the current equation and re-examine the nonlinear term.

The acoustoelectric current is the small D.C. shift in silicon current due to the presence of an acoustic wave on the lithium niobate. Writing the current equation with the assumed forms for E and n_s, we obtain:

$$J = e\mu(n_{s0} + n_{s1}^f)(E_0 + E_1) + eD\frac{\partial n_{s1}^f}{\partial z}.$$

We have, by taking the time average,

$$J_{AE} = \left\langle J_s - J_{s0} \right\rangle = e\mu \left\langle n_{s1}^f E_1 \right\rangle,$$

where n_{s1}^f, E_0, and $n_{s0}E_1$ are sinusoids, and hence have no time average.

Using the complex amplitudes from the linear analysis, we have:

$$J_{AE} = \frac{e\mu}{2} \mathrm{Re}\left\{ f\tilde{n}_{s1}\tilde{E}_1^* \right\}$$

$$= \frac{e\mu}{2} \mathrm{Re}\left\{ f\left(-\frac{k}{e\omega}\tilde{J}_1\right)\tilde{E}_1^* \right\}.$$

Substituting the conductivity function and $\frac{\omega}{k} \approx v_s$ (v_s = velocity of the acoustic wave), we have:

$$J_{AE} = \frac{\mu}{2v_s} \mathrm{Re}\left\{ f\sigma_s(\omega, k) \right\} \left|\tilde{E}_1\right|^2.$$

We may use a technique from the electrodynamics of dispersive media[14] to relate $\left|\tilde{E}_1\right|^2$ to the acoustic power flow. At each point

along z, the acoustic power lost must be the power dissipated in the semiconductor, since the acoustic medium itself is essentially lossless. A travelling wave which is attenuated has an imaginary part in its wave number k. The z-dependence of the acoustic power is then:

$$\left| \exp\ (-jkz) \right|^2 = \exp\ (2k_i z)$$

or

$$P_A = P_0 \exp\ (2k_1 z),$$

where P_A = acoustic sheet power, $P_0 = P_A$ at $z = 0$, and $k_i = \mathrm{Im}\left\{ k \right\} < 0$ for attenuation.

Using the effective conductivity function, we find that the power dissipated in the silicon is:

$$P_d = \tfrac{1}{2} \left| E_1 \right|^2 \mathrm{Re}\left\{ \sigma_s(\omega\ ,\ k) \right\} .$$

Now, using $\dfrac{dP_A}{dz} + P_d = 0$, we have:

$$2k_i P_A = -\tfrac{1}{2} \left| E_1 \right|^2 \mathrm{Re}\left\{ \sigma_s(\omega\ ,\ k) \right\} ,$$

or

$$\left| E_1 \right|^2 = \frac{-4k_i P_A}{\mathrm{Re}\left\{ \sigma_s(\omega\ ,\ k) \right\}} ,$$

The acoustoelectric current is therefore

$$J_{AE} = -\frac{\mu}{v_s} 2k_i P_A \frac{\mathrm{Re}\left\{ f\sigma_s(\omega\ ,\ k) \right\}}{\mathrm{Re}\left\{ \sigma_s(\omega\ ,\ k) \right\}} .$$

Since we are not using a magnetic field, we will always have

$$\left| \mathrm{Re}\left\{ \sigma_s(\omega\ ,\ k) \right\} \right| \gg \left| \mathrm{Im}\left\{ \sigma_s(\omega\ ,\ k) \right\} \right| .$$

From Appendix B it can be shown that $\mathrm{Im}\{f\} \leq \mathrm{Re}\{f\}$. Hence

$$\frac{\mathrm{Re}\{f\sigma_s(\omega, k)\}}{\mathrm{Re}\{\sigma_s(\omega, k)\}} \approx \mathrm{Re}\{f\}.$$

Hence we have

$$J_{AE} = -\frac{\mu}{v_s} 2k_i P_A \mathrm{Re}\{f\}.$$

This is just the sheet current density, at a point alongz, due to the acoustoelectric interaction. To relate this to the short-circuit terminal current in the actual experiment, we must solve a two-dimensional, rectangular-geometry, conduction problem. The acoustic beam is assumed to be well-defined of width w, so that the sheet acoustic power on the $LiNbO_3$ may be written as

$$P_A = \begin{cases} P_0 \exp(2k_i z), & |x| < w/2, \\ 0, & |x| > w/2, \end{cases}$$

where P_0 = sheet acoustic power at the silicon edge ($z = 0$), and k_i = attenuation per length due to interaction ($k_i < 0$).

A silicon sample, having width $b > w$ and length L, is positioned over the acoustic beam. (See Fig. 2.) This leads to the following conduction problem (with source $\vec{J}_s$):

$$\vec{J}_s = \begin{cases} \hat{i}_z J_{AE} = \hat{i}_z J_0 \exp(2k_i z), & |x| < w/2, \\ 0, & |x| > w/2, \end{cases} \quad 0 < z < L$$

and

$$J_0 = -\frac{\mu}{v_s} 2k_i P_0 \mathrm{Re}\{f\}.$$

The boundary conditions on V(z,x) are:

$$V(0, x) = V(L, x) = 0,$$

$$\frac{\partial V(z, \pm \frac{b}{2})}{\partial x} = 0,$$

and on the current:

$$I_{AE} = \int_{-b/2}^{b/2} \hat{i}_z \cdot \vec{J}_T(z,x)\, dx,$$

where $\vec{J}_T = \vec{J}_s + \vec{J}_1$ = total sheet current, source plus response.

Since this is a steady-state situation, the continuity equation gives

$$\nabla \cdot \vec{J}_T = 0 = \nabla \cdot \vec{J}_s + \nabla \cdot \vec{J}_1 \quad \text{or} \quad \nabla \cdot \vec{J}_1 = - \nabla \cdot \vec{J}_s.$$

From Ohm's law we have:

$$\vec{J}_1 = \sigma_d \vec{E} = - \sigma_d \nabla V \quad \text{or} \quad \nabla \cdot \vec{J}_1 = - \sigma_d \nabla^2 V.$$

So the appropriate differential equation is

$$\nabla^2 V = \frac{1}{\sigma_d} \nabla \cdot \vec{J}_s .$$

First, we find the particular solution. The transverse dependence of $\vec{J}_s$ may be expanded in a Fourier cosine series, and with careful choice of the fundamental period, the condition

$$\frac{\partial V}{\partial x} (z, x = \pm b/2) = 0$$

may be automatically be satisfied:

$$\vec{J}_s = \hat{i}_z J_0 \exp(2k_i z) \left[\frac{w}{b} + \sum_1^\infty \frac{2}{n\pi} \sin\left(\frac{n\pi w}{b}\right) \cos\left(\frac{n2\pi x}{b}\right) \right],$$

$$\nabla \cdot \vec{J}_s = 2k_i J_0 \exp(2k_i z) \left[\frac{w}{b} + \sum_1^\infty \frac{2}{n\pi} \sin\left(\frac{n\pi w}{b}\right) \cos\left(\frac{n2\pi x}{b}\right) \right].$$

Since we must satisfy $\nabla^2 V_P = \nabla \cdot \vec{J}_s$, the particular solution is assumed to be:

$$V_P = V_0 \exp(2k_i z) \left[a_0 + \sum_1^\infty a_n \cos\left(\frac{n2\pi x}{b}\right) \right].$$

Inserting this into the differential equation and matching coefficients, we find:

$$V_0 = \frac{J_0}{2k_i \sigma_d}, \quad a_0 = \frac{w}{b}, \quad a_n = \frac{2}{n\pi} \sin\left(\frac{n\pi w}{b}\right) \frac{(2k_i)^2}{(2k_i)^2 - \left(\frac{n2\pi}{b}\right)^2}.$$

A homogeneous solution must now be added to match boundary conditions. The choice of solution to $\nabla^2 V = 0$ in this configuration is:

$$V_H = V_{H0} + \frac{V_{H1} z}{L} + \sum_1^\infty \cos\left(\frac{n2\pi x}{b}\right) \left[A_n \cosh\left(\frac{n2\pi z}{b}\right) + B_n \sinh\left(\frac{n2\pi z}{b}\right) \right].$$

Using $V_P + V_H = 0$ at $z = 0$, we find $V_{H0} = - V_0 a_0$ and $A_n = - V_0 a_n$. Using the same boundary condition at $z = L$ yields

$$V_{H1} = V_0 a_0 (1 - \exp(2k_i L)) \quad \text{and} \quad B_n = V_0 a_n \left[\frac{\cosh\left(\frac{n2\pi L}{b}\right) - \exp(2k_i L)}{\sinh\left(\frac{n2\pi L}{b}\right)} \right].$$

We may now determine I_{AE} by performing the previously indicated integration. The most convenient path of integration is to hold $z = 0$:

$$I_{AE} = \int_{-b/2}^{b/2} \hat{i}_z \cdot K_{AE} \Big|_{z=0} dx - \sigma_d \int_{-b/2}^{b/2} \left(\frac{\partial V}{\partial z}\right)_{z=0} dx$$

$$= J_0 w - \sigma_d \left(\frac{J_0 w}{\sigma_d} + \frac{J_0 w}{2k_i \sigma_d L} (1 - \exp(2k_i L)) \right)$$

$$= - \frac{J_0}{2k_i} \frac{w}{L} (1 - \exp(2k_i L)).$$

But

$$J_0 = - \frac{\mu}{v_s} 2k_i P_0 \, \mathrm{Re}\{f\}$$

and

$$P_0 w(1 - \exp(2k_i L)) = P_D,$$

the power dissipated in the silicon. Therefore we have:

$$I_{AE} = \frac{\mu}{v_a} \frac{P_0}{L} \mathrm{Re}\{f\}.$$

APPENDIX B

TRAPPING FACTOR

Here we derive the trapping factor, f, which is the ratio of mobile (or free) A.C. bunched-electron density to total A.C. bunched-electron density. The particular situation considered is for electrons in an accumulation layer on N-type silicon; other situations would use a very similar analsis.

Traps are considered to be distributed throughout the energy gap, and in communication with free electrons in the accumulation layer of sheet density n_s. $N_{ss}(E)$ is the sheet density per joule of surface states (traps) at energy E. The trapped electron sheet density per electron volt is

$$\frac{dn_t}{dE} = N_{ss}(E)F(E),$$

where $F(E)$ is the distribution function. (n_t is obviously the total trapped electron sheet density.)

We may formulate the following dynamics for traps at energy E:

$$\frac{d}{dt}\left(\frac{dn_t}{dE}\right) = C(E)n_s(1 - F(E))N_{ss}(E) - e(E)F(E)N_{ss}(E).$$

The net rate of change of sheet density of electrons trapped at energy E is the rate of capture less the expulsion rate. The rate of capture is the capture probability of an electron by a trap ($C(E)$) times the number of empty traps available ($(1 - F(E))N_{ss}(E)$) times the number of electrons available (n_s). The expulsion rate is the expulsion probability for an electron in a trap ($e(E)$) times the number of full

traps ($F(E)N_{ss}(E)$).

At equilibrium we have

$$n_s = n_{s0},$$

$$F(E) = F_0(E) \qquad \text{(the Fermi factor)},$$

and

$$\frac{d}{dt}\left(\frac{dn_t}{dE}\right) = 0.$$

This gives

$$e(E) = C(E)n_{s0}\left(\frac{1 - F_0(E)}{F_0(E)}\right).$$

We may now linearize for small signals and assume $\exp(j\omega t)$ time dependence:

$$j\omega \frac{d\tilde{n}_{t1}}{dE} = C(E)N_{ss}(E)\left[\tilde{n}_{s1}(1 - F_0(E)) - n_{s0}\tilde{F}_1(E) - n_{s0}(1 - F_0(E))\frac{\tilde{F}_1(E)}{F_0(E)}\right],$$

$$j\frac{\omega}{C(E)}\frac{d\tilde{n}_{t1}}{dE} = N_{ss}(E)(1 - F_0(E))\tilde{n}_{s1} - \frac{n_{s0}}{F_0(E)}\tilde{F}_1(E)N_{ss}(E).$$

But

$$\tilde{F}_1(E)N_{ss}(E) = \frac{d\tilde{n}_{t1}}{dE}$$

gives

$$\frac{d\tilde{n}_{t1}}{dE} = \frac{N_{ss}(E)(1 - F_0(E))\tilde{n}_{s1}}{\frac{j\omega}{C(E)} + \frac{n_{s0}}{F_0(E)}},$$

$$\tilde{n}_{t1} = \frac{\tilde{n}_{s1}}{n_{s0}} \int_{E_v}^{E_c} \frac{N_{ss}(E)F_0(E)(1 - F_0(E))\,dE}{1 + \frac{j\omega F_0(E)}{C(E)n_{s0}}}.$$

We seek the trapping factor

$$f = \frac{\tilde{n}_{s1}}{\tilde{n}_{s1} + \tilde{n}_{t1}},$$

but it is easier to evaluate

$$\frac{1}{f} - 1 = \frac{\tilde{n}_{t1}}{\tilde{n}_{s1}} .$$

So

$$\frac{1}{f} - 1 = \frac{1}{n_{s0}} \int_{E_v}^{E_c} \frac{N_{ss}(E)F_0(E)(1 - F_0(E))\, dE}{1 + \frac{j\omega F_0(E)}{C(E)n_{s0}}} .$$

In order to perform this integration we make three assumptions:

1) The limits E_c, E_v may be moved to $\pm\infty$ with essentially no effect. This is true because $F(1 - F)$ goes to zero rapidly as the energy differs from the Fermi energy, E_F.

2) $C(E) = C$, constant.

3) $N_{ss}(E)$ varies slowly compared to $F(1 - F)$ around the Fermi energy.

Assumptions (2) and (3) have been shown to be valid in surface-state investigations.

We now have

$$\frac{1}{f} - 1 = \frac{N_{ss}(E_F)}{n_{s0}} \int_{-\infty}^{\infty} \frac{F_0(E)(1 - F_0(E))\, dE}{1 + \frac{j\omega F_0(E)}{Cn_{s0}}} .$$

For very low frequencies f obviously approaches an asymptote, f_0:

$$\lim_{\omega \to 0} \left(\frac{1}{f} - 1\right) = \frac{1}{f_0} - 1 = \frac{N_{ss}(E_F)}{n_{s0}} \int_{-\infty}^{\infty} F_0(E)(1 - F_0(E)\, dE$$
$$= \frac{kTN_{ss}(E_F)}{n_{s0}} .$$

At arbitrary frequency, recognizing that $F_0(E)(1 - F_0(E))\, dE = kT\, dF_0$, we have:

$$\frac{1}{f} - 1 = \frac{kTN_{ss}(E_F)}{n_{s0}} \int_0^1 \frac{dF_0}{1 + \frac{j\omega F_0}{Cn_{s0}}} = \left(\frac{1}{f_0} - 1\right) \frac{Cn_{s0}}{j\omega} \ln\left(1 + \frac{j\omega}{Cn_{s0}}\right) .$$

If we define $\tau \equiv \frac{1}{Cn_{s0}}$, we have:

$$\left(\frac{1}{f} - 1\right) = \left(\frac{1}{f_0} - 1\right) \left[\frac{\ln(1 + j\omega\tau)}{j\omega\tau}\right] .$$

APPENDIX C

SHEET MODEL

We wish to model the accumulation layer as a sheet conductance. The neglect of bulk conduction compared to conduction in the accumulation layer is justified over a wide range of sheet densities because the silicon we are using has $\sim 10^{11}$ electrons/cm^3 ($n_i = 10^{10}$/cm^3 for Si). The main consideration in the sheet model is that the sheet thickness be small with respect to the acoustic wavelength, so that variations in the acoustic field strength with depth need not be considered.

Consider the band structure associated with the accumulation layer on N-type silicon. In the discussion which follows, E_c = energy of conduction band edge, E_F = Fermi energy, E_i = intrinsic energy level, and E_v = energy of valence band edge.

The electrostatic potential is related to band energies by

$$\phi(x) = - e(E_i(x) - E_i(\infty)),$$

where $\phi(x)$ = electrostatic potential at x, $E_i(x)$ = intrinsic energy level at x, $E_i(\infty)$ = bulk intrinsic energy level, and e = electronic charge magnitude.

Measuring potential in units of kT/e ($U(x) = e\phi(x)/kT$), the usual semiconductor equations become:

$$p = n_i \exp (U_F - U),$$

$$n = n_i \exp (U - U_F),$$

and

$$\rho = e(p - n + N_D - N_A),$$

where p = hole density, n = electron density, n_i = intrinsic carrier density, ρ = charge density, N_D = donor density, and N_A = acceptor density.

At this point we may neglect holes, since we are considering N-type material with only an accumulated surface. Let the compensated donor density be $N_O = N_D - N_A$. In the bulk ($x \rightarrow \infty$) the charge density must vanish:

$$n(\infty) = N_O = n_i \exp(U_F).$$

Poisson's equation in one dimension is

$$\frac{d^2\phi}{dx^2} = -\frac{\rho}{\epsilon} \quad \text{or} \quad \frac{d^2U}{dx^2} = -\frac{e}{kT\epsilon}\rho;$$

so

$$\frac{d^2U}{dx^2} = -\frac{e^2 n_O}{kT\epsilon}(1 - \exp(U)).$$

Multiplying by 2(dU/dx), we have

$$2\frac{dU}{dx}\frac{d^2U}{dx^2} = \frac{d}{dx}\left(\frac{dU}{dx}\right)^2 = -\frac{e^2 n_O}{kT\epsilon} 2\frac{dU}{dx}(1 - \exp(u)).$$

Using

$$\frac{kT\epsilon}{e^2 n_O} = \lambda_D^2,$$

the intrinsic Debye length, and the fact that U and $\frac{dU}{dx}$ must vanish in the bulk, we obtain

$$\int_\infty^x \frac{d}{dx}\left(\frac{du}{dx}\right)^2 dx = \left(\frac{du}{dx}\right)^2 = -\frac{2}{\lambda_D^2}\int_0^U (1 - \exp(U))\, dU$$

$$= \frac{2}{\lambda_D^2}(\exp(U) - U - 1).$$

Choosing the appropriate sign for the square root, we have

$$\frac{dU}{dx} = -\frac{\sqrt{2(\exp(U) - U - 1}}{\lambda_D} .$$

Integrating again, we get:

$$\int_0^x \frac{\sqrt{2}\, dx}{\lambda_D} = \sqrt{2}\frac{x}{\lambda_D} = \int_{U_s}^{U} \frac{dU}{\sqrt{\exp(U) - U - 1}} .$$

If we restrict our attention to $U > 3$, we may neglect U and 1 with respect to the exponential and obtain:

$$\sqrt{2}\ \frac{x}{\lambda_D} = \int_{U_s}^{U} \exp(-U/2)\, dU$$

$$= 2(\exp(-U/2) - \exp(-U_s/2)),$$

but

$$\frac{n}{n_0} = \exp(U);$$

$$\frac{x}{\sqrt{2}\lambda_D} = \sqrt{\frac{n_0}{n}} - \sqrt{\frac{n_0}{n_{0s}}},$$

where $n_{0s} = n_i(\exp(U_s))$ = peak electron volume density at the surface;

$$1 + \frac{x}{\sqrt{2}\lambda_D}\sqrt{\frac{n_{0s}}{n_0}} = \sqrt{\frac{n_{0s}}{n}} ;$$

and

$$n = \frac{n_{0s}}{\left(1 + \frac{x}{\sqrt{2}\lambda_D}\sqrt{\frac{n_{0s}}{n_0}}\right)^2}.$$

Obviously this expression is wrong, as x becomes large because n approaches zero instead of n_0. This is because (U + 1) was neglected in solving the differential equation. If that term were included, it would cause a slower fall of n with x, finally approaching n_0.

For the densities we are considering, the slowly decreasing tail of the density may be ignored, along with the bulk density, compared to the accumulation layer. From here on, the n(x) derived will be considered to be the true electron density in the accumulation layer.

The sheet density of the accumulation layer is:

$$n_s = \int_0^\infty n\,dx = \int_0^\infty \frac{n_{0s}\,dx}{\left(1 + \frac{x}{\sqrt{2}\lambda_D}\sqrt{\frac{n_{0s}}{n_0}}\right)^2}$$

$$= \sqrt{2}\lambda_D \sqrt{n_{0s}n_0} \int_0^\infty \frac{dx'}{(1 + x')^2}$$

$$= \sqrt{2}\lambda_D \sqrt{n_{0s}n_0} \left[\frac{-1}{1 + x'}\right]_0^\infty$$

$$= \sqrt{2}\lambda_D n_0 \exp\,(U_s/2).$$

If we consider the sheet thickness, d_s, to be the value of x such that 90% of the electron sheet density is between 0 and x, we find:

$$\int_{d'}^\infty \frac{dx'}{(1 + x')^2} = \frac{1}{1 + d'} = .1, \qquad d' = 9,$$

and

$$d_s = 9\sqrt{2}\lambda_D \sqrt{\frac{n_0}{n_{0s}}} = 9\sqrt{2}\lambda_D \exp\,(-U_s/2).$$

Using

$$\epsilon = 12\,\epsilon_0, \quad n_0 = 10^{11}\ \text{cm}^{-3}, \quad \frac{kT}{e} = 0.026\ \text{V},$$

and

$$e = 1.6 \times 10^{-19}\ \text{coul},$$

we have:

$$\lambda_D = 13\ \mu,$$

$$n_s = 18.4 \times 10^7 \exp\,(U_s/2)\ \text{cm}^{-2},$$

$$d_s = 166 \exp\,(-U_s/2)\ \mu\text{m}.$$

We require the sheet thickness to be much less than the acoustic wavelength. At 166 MHz,

$$\lambda = \frac{3485\ \text{m/sec}}{166\ \text{MHz}} = 21\,\mu\text{m}.$$

If we choose d_s max $\approx 2\,\mu$m, the minimum surface potential is $U_s = 8.8$. This justifies the earlier assumption of avoiding potentials $U < 3$. The peak density is exp (8.8) = 6.7×10^3 times the bulk. This corresponds to a sheet electron density of 1.5×10^{10} cm^{-2}, which is the minimum sheet density encountered in the experiment.

APPENDIX D

CALCULATIONS

1) Accumulation-layer sheet conductance may be found by subtracting the conductance due to bulk and back-side carriers from the total sheet conductance of the sample. The sum of bulk and back-side conductances may be determined from the sample resistance when V_T corresponds to the flat-band condition but, due to oxide charge and metal-semiconductor work-function difference, we do not know this value of V_T. If, instead, we measure the maximum resistance (vs. V_T), we will determine the minimum sheet conductance, which is slightly less than the flat-band value by the amount the front side is depleted). This difference is small to begin with and becomes less important as the total sheet conductance grows larger, so this is the sheet conductance we will subtract for bulk and back-side correction.

For sample BB49C, Run #1, we have

$$\sigma_{d\ min} = \left(\frac{L}{w}\right) \frac{1}{R_{max}}$$

with

$$\frac{L}{w} = \frac{400\ mil}{120\ mil} = \frac{10}{3}$$

and

$$R_{max} = 1.88\ M\Omega \quad \text{at } V_T = -260\ V,$$

$$d\ min = 1.77 \mu\mho\ .$$

So, for this sample, at other bias, we have

$$\sigma_d = \left(\frac{10}{3}\right) \frac{1}{R} - 1.77 \mu\mho\ .$$

2) Sheet electron density may be determined through the sheet conductance or the silicon-to-field-plate capacitance.

Since we know that $\sigma_d = e\mu n_s$ and $e = 1.9 \times 10^{-19}$ coul, and we calculate μ and σ_d from the experiment, we may also calculate the electron sheet density as

$$n_{s\mu} = \frac{\sigma_d}{e\mu}.$$

Arguing that the structure is a linear parallel-plate capacitor, we have

$$\Delta n_s = \frac{C}{A} \Delta V_T \qquad \text{with } C = \frac{\epsilon_\perp A}{d}$$

or

$$\Delta n_s = \frac{\epsilon_\perp}{d} \Delta V_T,$$

where $\epsilon_\perp$ = dielectric permittivity normal to $LiNbO_3$ surface; A = capacitor area; d = separation of Si surface from field plate $\sim LiNbO_3$ thickness.

In order to correct for fringing effects, a two-dimensional conduction analog (silver-paint electrodes on conductive "Teledeltos" paper) was used to find the ratio of true capacitance to parallel-plate capacitance; $2.295 \approx 2.3$ was the result. Since, due to fringing, n_s is not uniform, the n_s found will be an average over the area. This capacitance method can only determine changes in the sheet charge density because at zero bias the sheet charge is unknown. We shall use, to set the absolute sheet electron density, a (low) value calculated from the mobility measurement. For BB49C, Run #1,

$$n_s\mu(V_T = -100\ V) = \frac{5.44\,\mu\upsilon}{(1.6 \times 10^{-19}\ \text{coul})(856\ \text{cm}^2/\text{V} \cdot \text{sec})} = 3.63 \times 10^{10}\ \text{cm}^{-2};$$

so

$$n_{sc} = 2.3 \frac{\epsilon_i}{d} (V_T + 100\ V) + 3.63 \times 10^{10}\ cm^{-2}$$

$$= \frac{(2.3)(84 \times 8.85 \times 10^{-14}\ f/cm)}{(0.25\ cm)} (V_T + 100\ V) + 3.63 \times 10^{10}\ cm^{-2},$$

and

$$n_{sc} = (0.684(V_T + 100\ V) + 3.63) \times 10^{10}\ cm^{-2}.$$

Here the second subscript on n_s (μ or c) refers to the method of determination (mobility or capacitance).

3) The power incident at the silicon edge is estimated from the nominal input power. The power at the silicon edge, P_0, is the power read by the power meter less the attenuator and input-transducer losses. (The losses through the stub tuner are negligible.) The delay-line loss with no silicon present, 8.45 db, is the loss due to the two transducers (assumed equal) and an estimated 0.85 db diffraction loss. Therefore the input-transducer insertion loss is estimated to be 3.80 db. With the power meter set at -1 dbm, the power is

$$P_0 = -1 - P_{Att} - 3.80\ db,$$

where P_{Att} is the attenuator insertion loss - 0.31, 10.32, 20.27 db.

Converting back to a linear power scale, we have:

Nominal	Actual
- 1 db	3.112 W
- 11 db	30.76 W
- 21 db	308.3 W

(This P_0 is the same as that used in Appendix A.)

4) The fraction of P_0 used (the $(1 - \exp(2k_i L))$ of Appendix A) may be determined by measuring the excess insertion loss of the delay line due to the presence of the silicon. This excess loss is just $\exp(2k_i L)$ measured in db. If P_{DL} is the total insertion loss of the delay line with the silicon in place, we have

$$1 - \exp(2k_i L) = 1 - \exp(-0.23(P_{DL} - 8.45)).$$

5) The mobility may be calculated from the acoustoelectric current as

$$I_{AE} = \frac{V_{AE}}{R} = \frac{\mu}{v_s}\frac{P_D}{L} \qquad \text{or} \qquad \mu = \frac{v_s L\, V_{AE}}{RP_0(1 - \exp(2k_i L))}.$$

6) Several data points and calculated parameters from Run #1 on BB49C are presented in Table 1.

TABLE 1

V_T	R	P_{Loss}	P_0	V_{AE}	μ	σ_d	$n_{s\mu}$	n_{sc}
(V)	($M\Omega$)	(db)	(μW)	(mV)	($\frac{cm^2}{V \cdot sec}$)	($\mu\mho$)	(10^{10} cm^{-2})	
-100	0.462	30.2	3.112	3.78	936	5.44	3.63	3.63
0	0.282	25.6	30.76	20.6	856	10.05	7.34	7.98
100	0.205	19.4	30.76	13.2	805	14.49	11.25	12.33
200	0.164	17.3	30.76	9.45	762	18.55	15.21	16.69
400	0.120	15.3	30.76	5.60	676	26.00	24.04	25.41
600	0.099	14.5	30.76	3.68	568	31.90	35.10	34.18

NOTES

1. D. L. White, J. Appl. Phys. 33, 2547 (1963).

   A. R. Hutson, J. H. McFee, and D. L. White, Phys. Rev. Letters 7, 237 (1961).

2. J. H. Collins, K. M. Laken, C. F. Quate, and H. J. Shaw, Appl. Phys. Letters 13, 314 (1968).

   A. Bers and B. E. Burke, Appl. Phys. Letters 16, 300 (1970).

   A. Bers, Invited Proc. 1970 Ultrasonics Sym., IEEE Publication 70 C 69 80, New York, pp. 138-172 (1970).

3. B. E. Burke, A. Bers, H. I. Smith, R. A. Cohen, and R. W. Mountain, Proc. IEEE 58, 1775 (1970).

4. K. A. Ingsbrigtsen, J. Appl. Phys. 41, 454 (1970).

   J. H. Cafarella and A. Bers, R. L. E. Quarterly Prog. Report 104, 217 (1972), M. I. T., Cambridge, Mass.

   M. Yamanishi and K. Yoshida, Bull. Univ. Osaka Pref. 18, 365 (1969).

5. W. Shockley and W. T. Read, Jr., Phys. Rev. 87, 835 (1952).

6. A. S. Grove, B. E. Deal, E. H. Snow, and C. T. Sah, Sol.-St. Elec. 8, 145 (1965).

   D. M. Brown and P. V. Gray, J. Elec. Soc. 115, 760 (1968).

7. C. A. A. J. Greebe, IEEE Trans. Son. Ultrason. SU-13, 54 (1966).

   A. R. Moore and R. W. Smith, Phys. Rev. 138, A1250 (1965).

8. A. Many, Y. Goldstein, and N. B. Grover, Semiconductor Surfaces, John Wiley and Sons, New York, 1965, Ch. 9.

9. O. Leistiko, Jr., A. S. Grove, and C. T. Sah, IEEE Trans. El. Dev. ED-12, 248 (1965).

10. T. L. Szabo and A. J. Slobodnik, IEEE Trans. Son. Ultrason. (to be published).

11. E. H. Nicollian and A. Goetzberger, The Bell System Tech. Journal XLVI, 1055 (1967).

12. J. R. Schrieffer, Phys. Rev. 97, 641 (1955).

13. A. B. Fowler, F. Fang, and F. Hochberg, IBM Journal, 427 (Sept. 1964).

14. A. Bers, Course Notes, M. I. T., Cambridge, Mass. (1964) unpublished.

W. P. Allis, S. J. Buchsbaum, and A. Bers, Waves in Anisotropic Plasmas, M. I. T. Press, Cambridge, Mass., 1963.

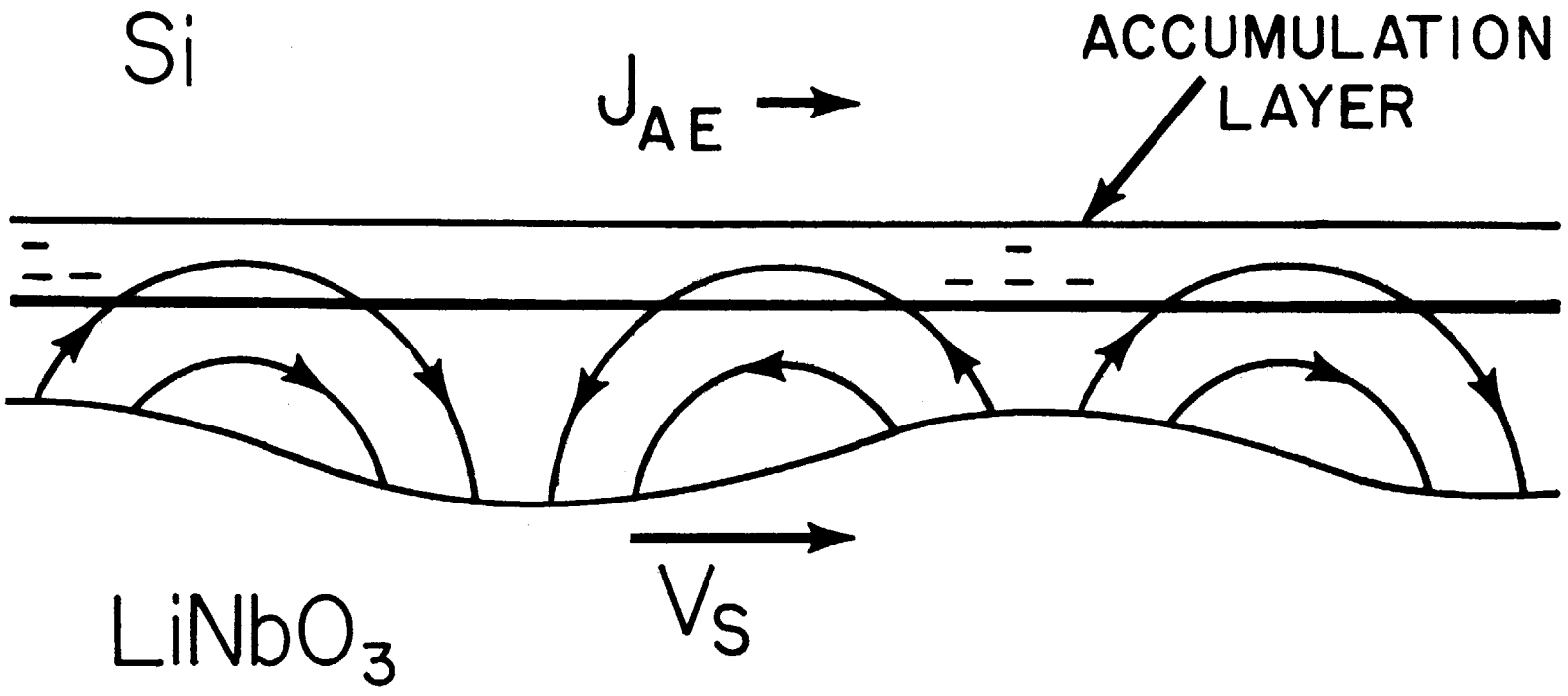

$$I_{AE} = \frac{\mu}{V_S} \frac{P_D}{L} \text{ Re } \{f\}$$

Fig. 1 Accumulation layer interaction.

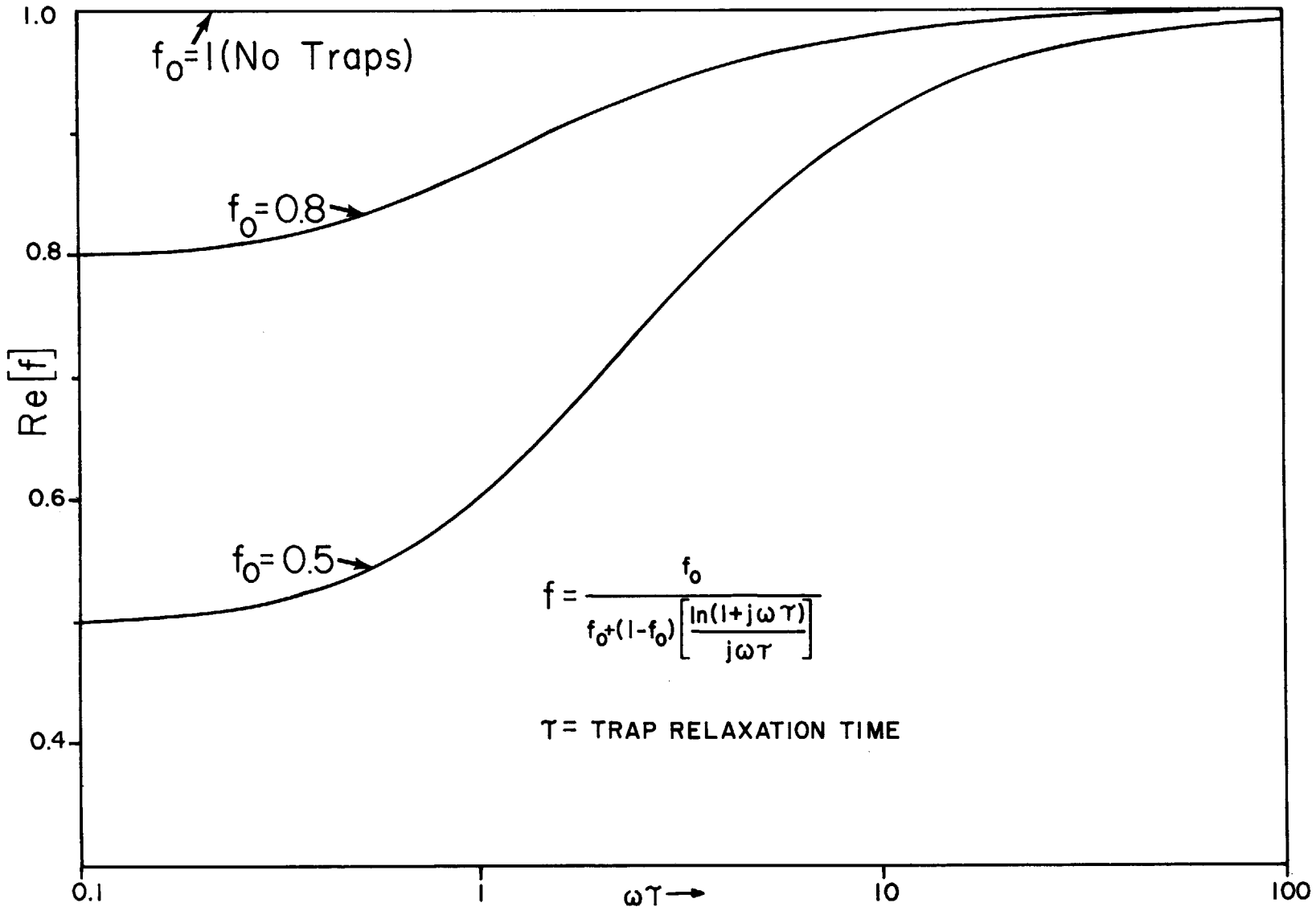

Fig. 2 Real part of the trapping factor.

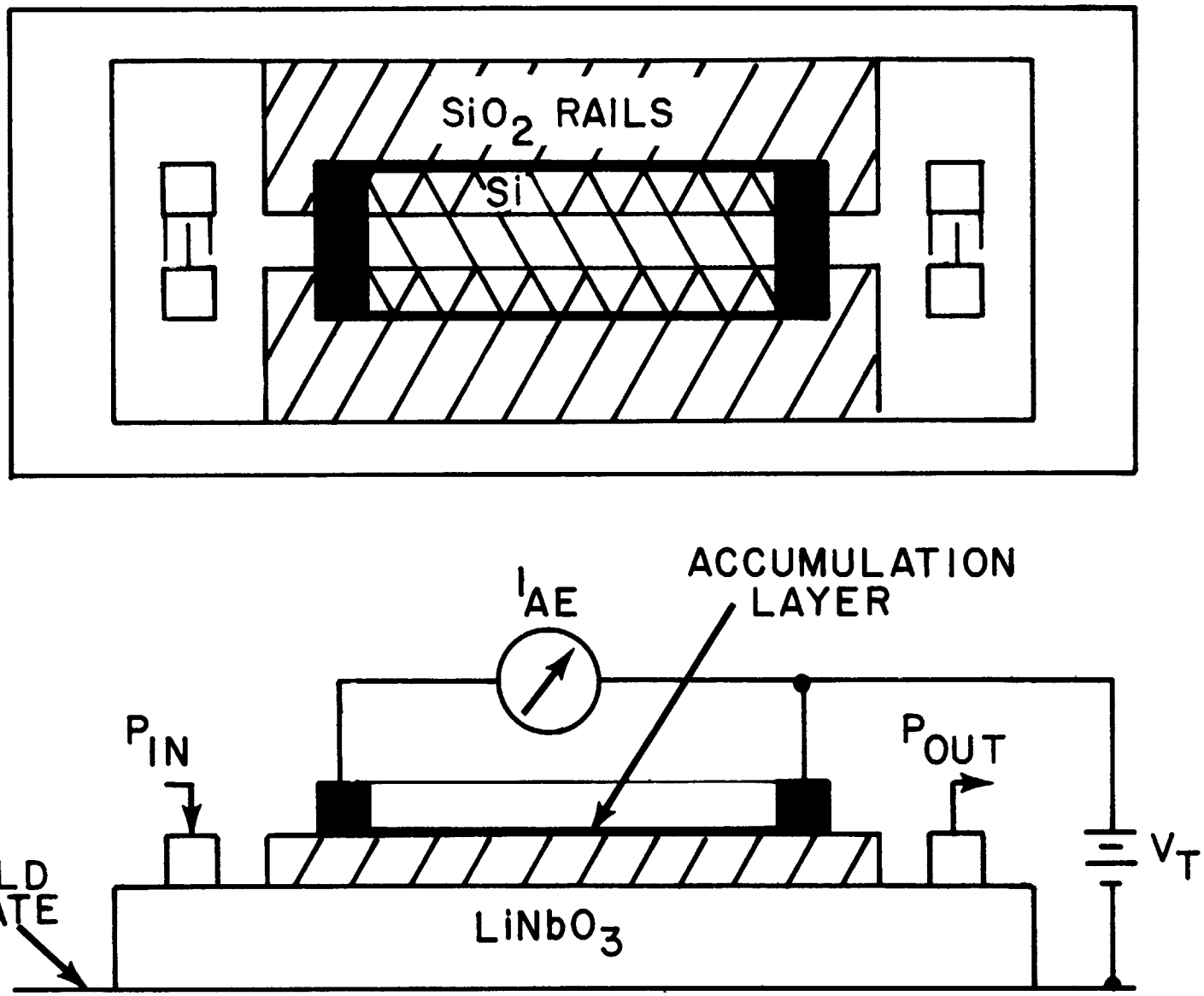

Fig. 3 Configuration of the experiment.

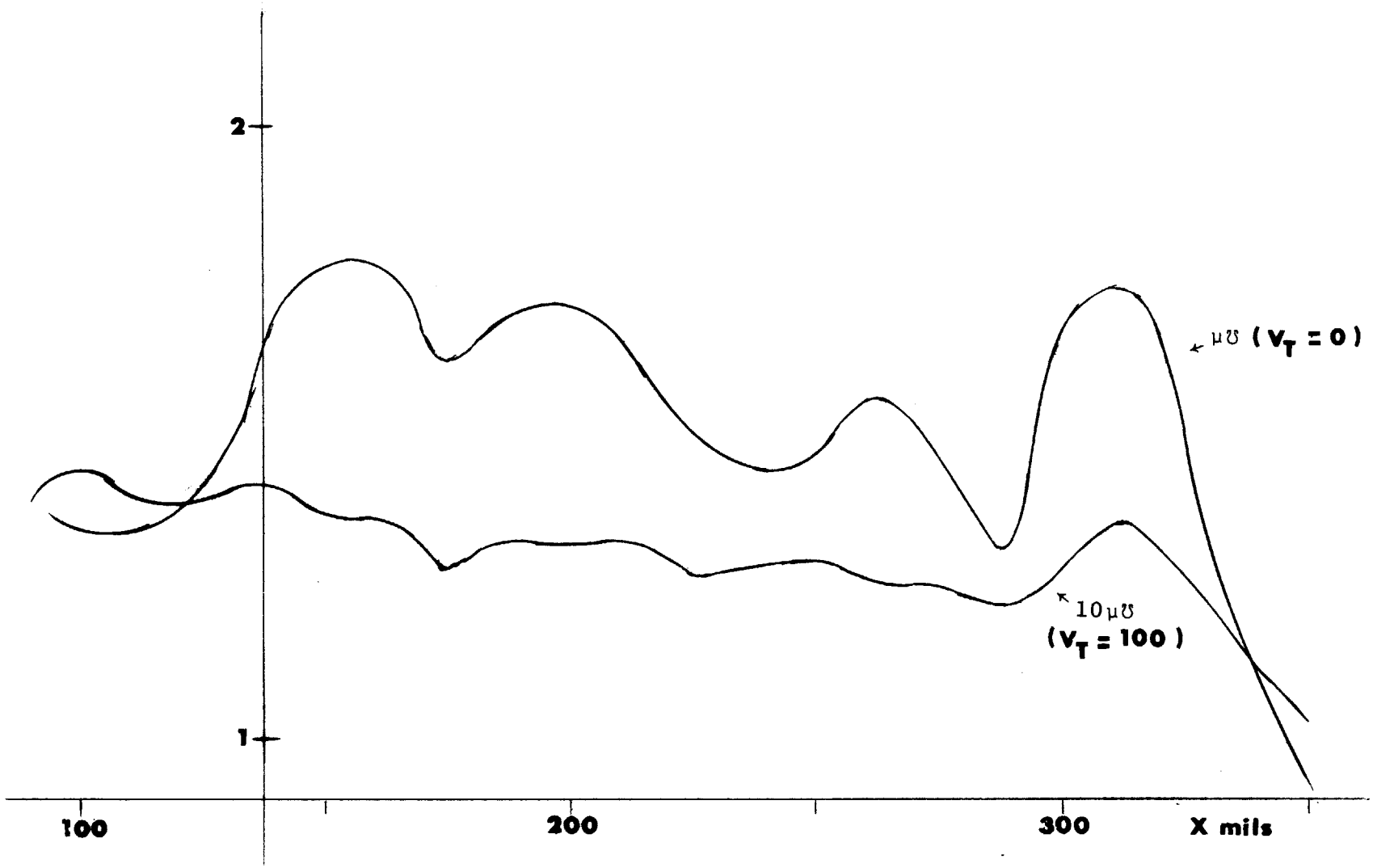

Fig. 4 Sheet conductivity vs. length.

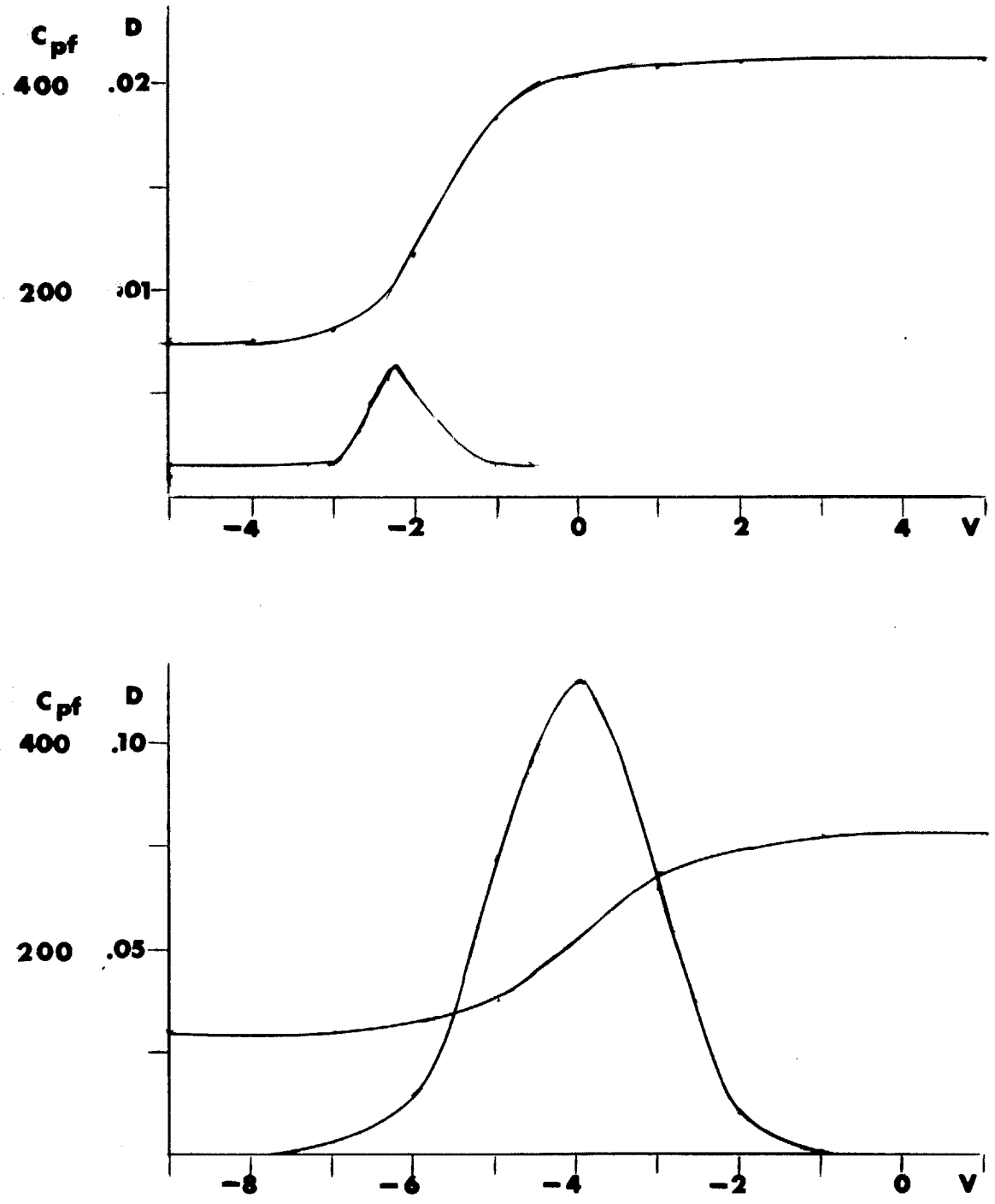

Fig. 5 M.O.S. conductance results on monitor samples.

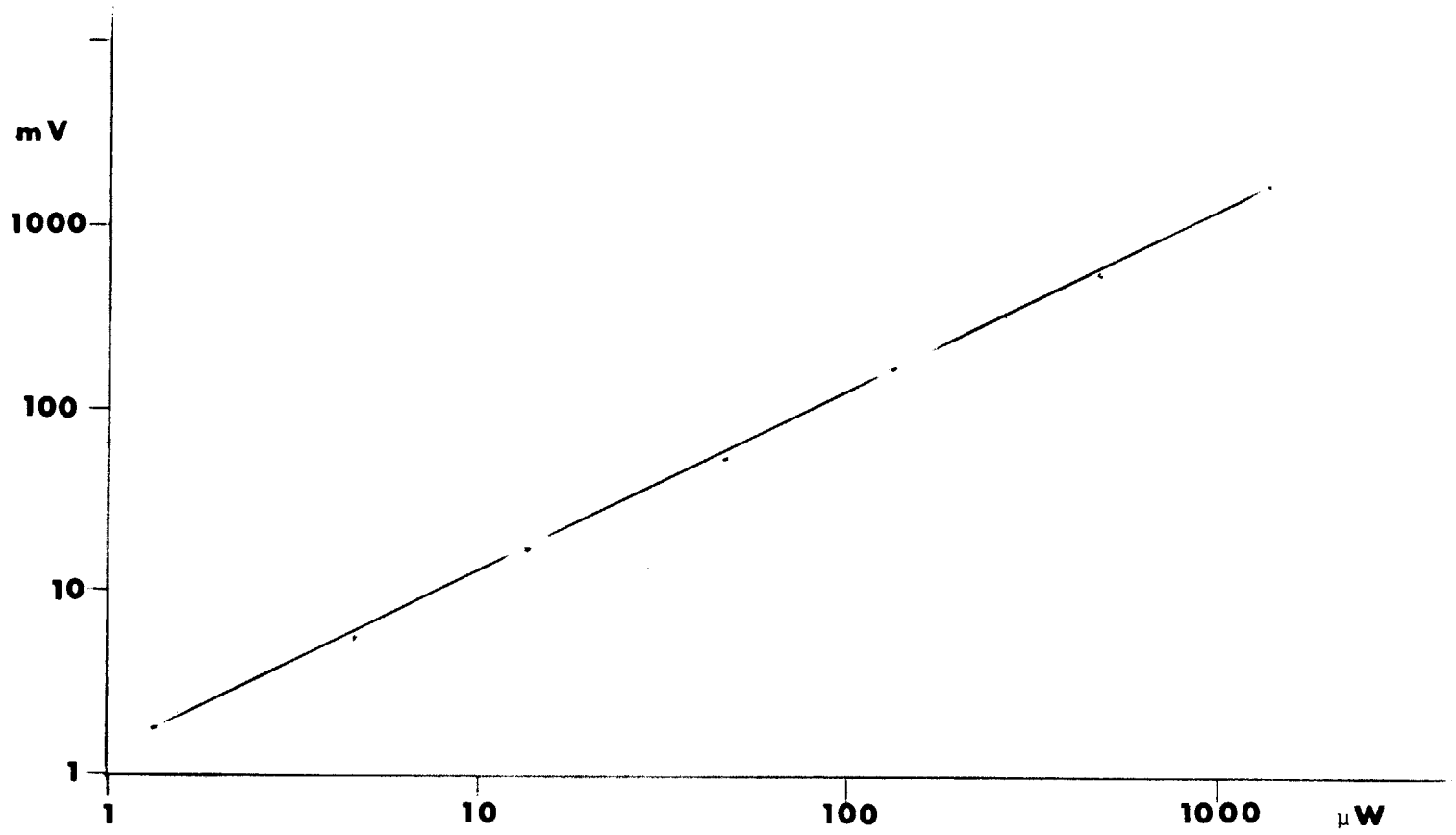

Fig. 6 Acoustoelectric voltage linearity with power.

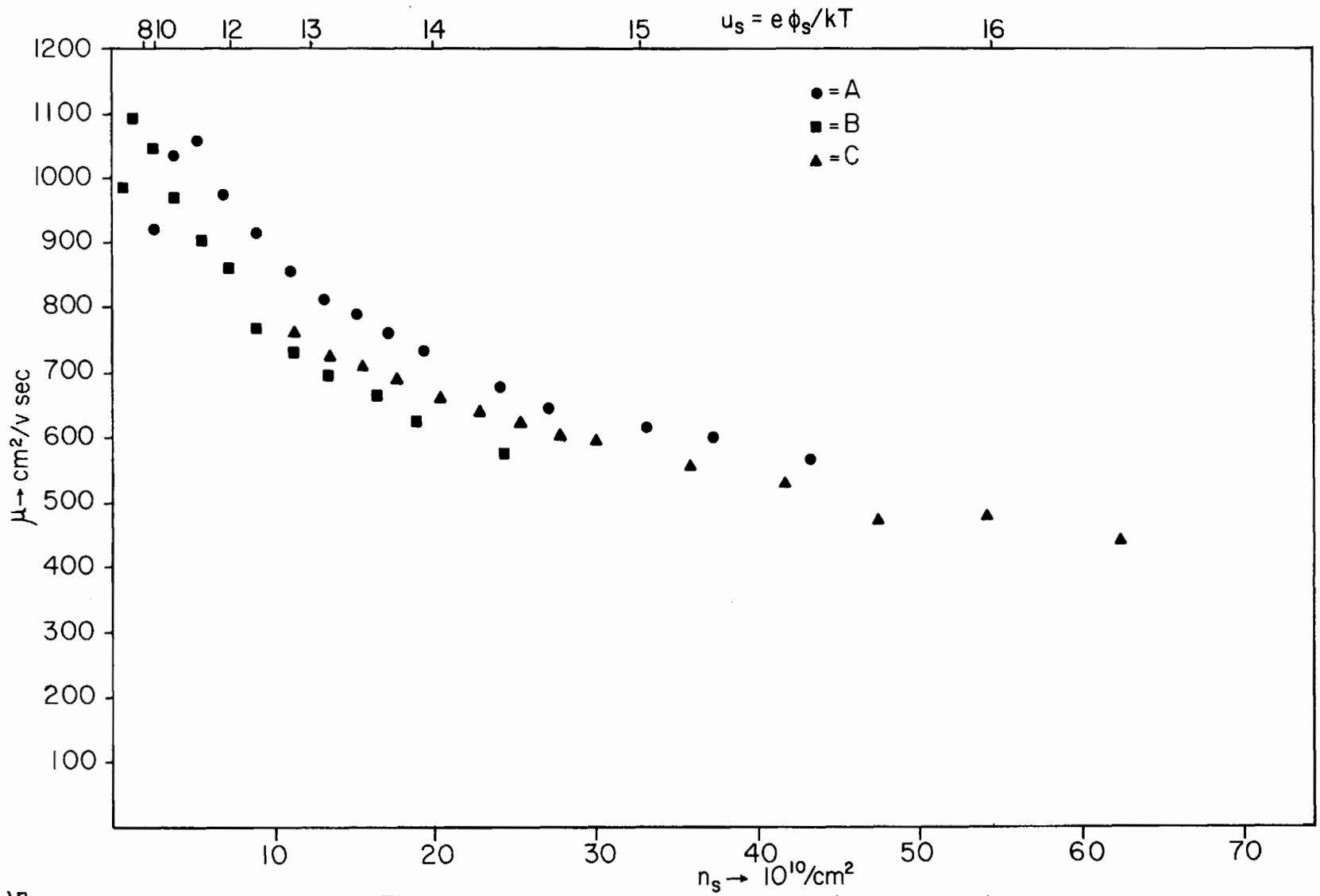

Fig. 7 Mobility vs. band-bending (and density).

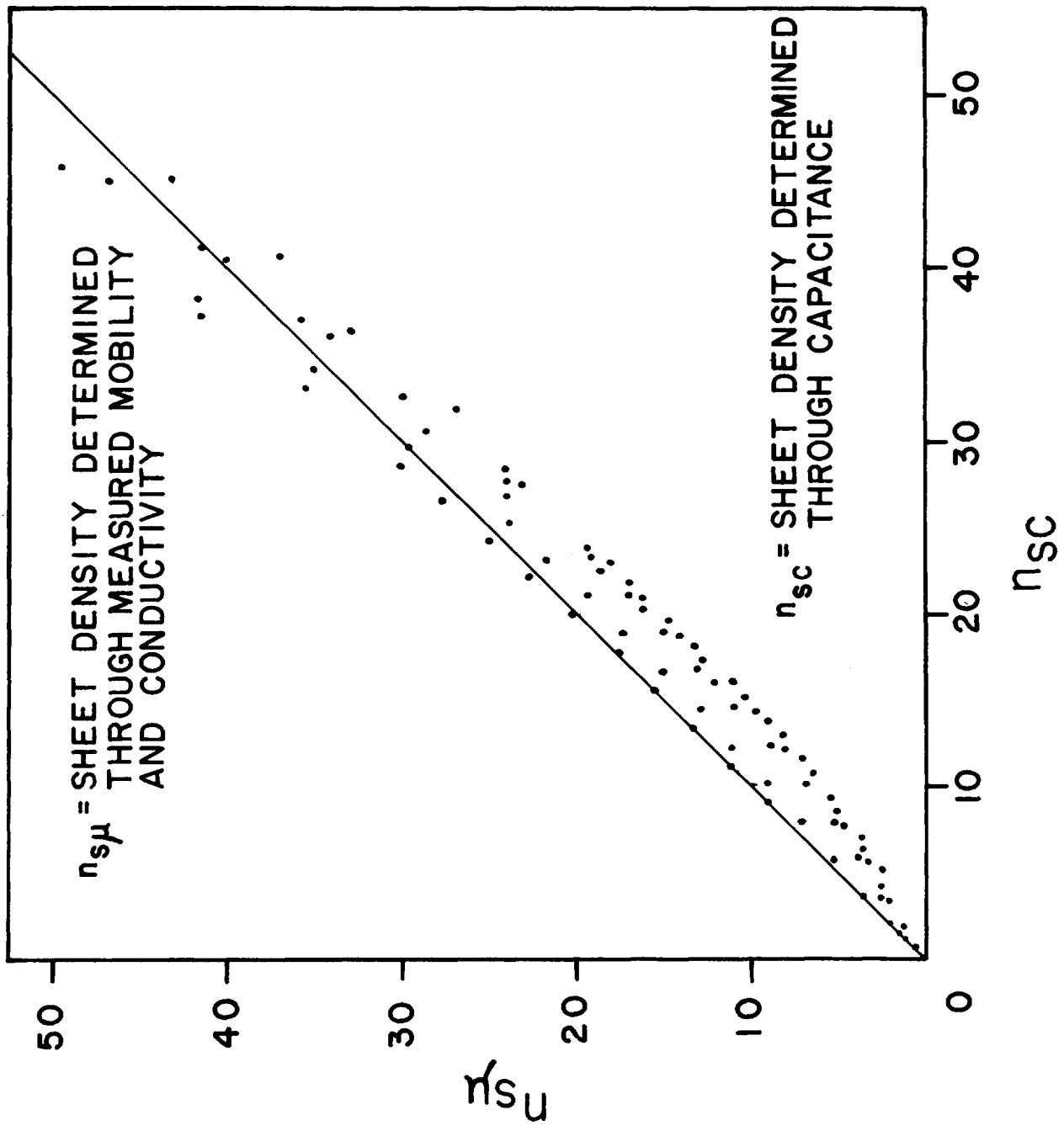

Fig. 8 Sheet electron density determined by capacitance and mobility.

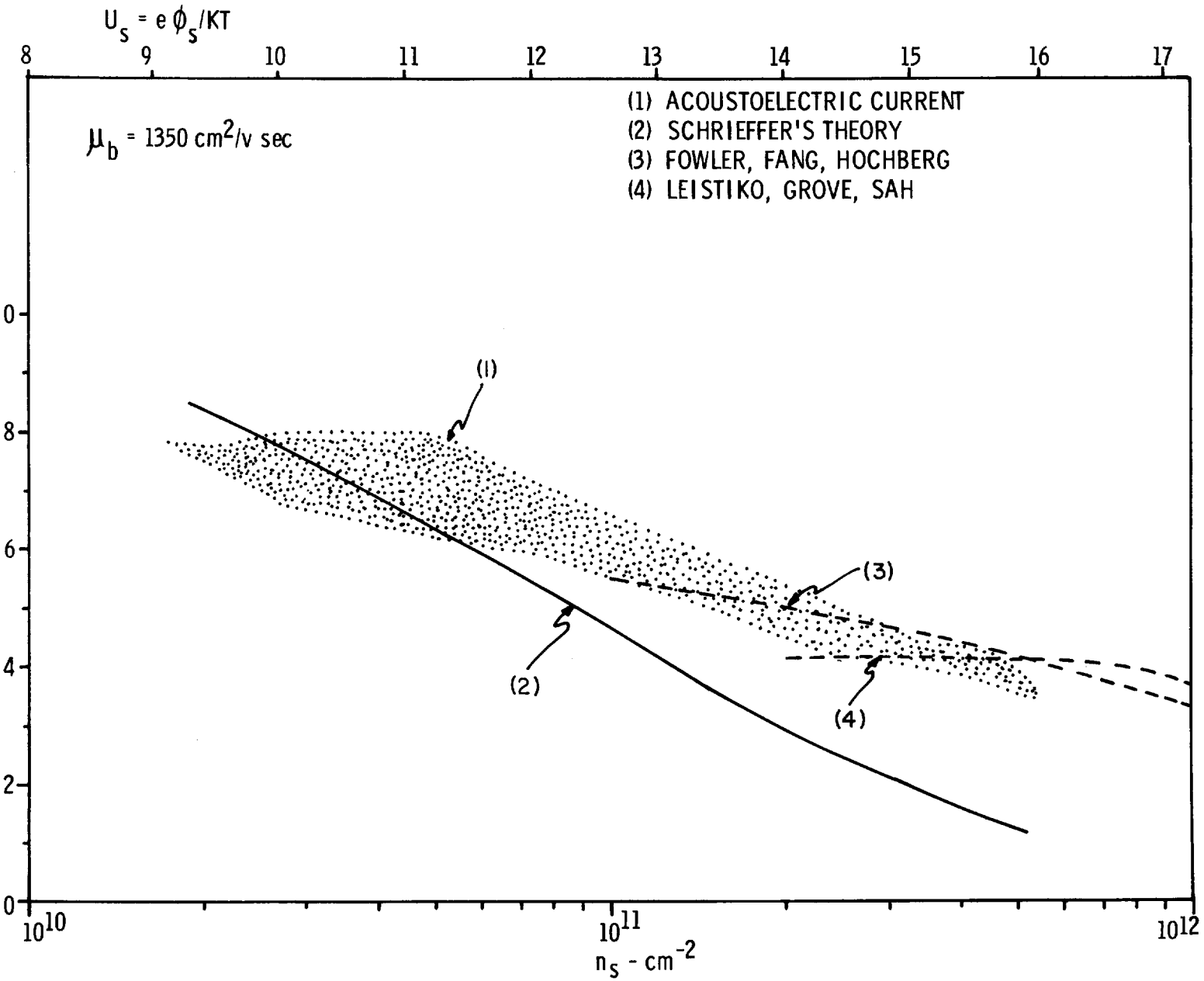

Fig. 9 Measured mobilities compared to theoretical and other experimental values.

ACKNOWLEDGMENTS

I would like, at this time, to thank the people who helped me complete this thesis, although I could not possibly name them all. First, to Professor Abraham Bers I extend my gratitude for his persistence as my thesis advisor. His guidance saw me through not only the theoretical development of the acoustoelectric current experiment, but also through most of my background in electrodynamics. To Dr. Barry Burke my thanks for his assistance in developing the experiment at Lincoln Laboratory. For his support and interest during the experiment I thank Dr. Ernest Stern, leader of group 86, Lincoln Laboratory.

My appreciation also for technical assistance to the members of group 86, especially Mr. John Alusow.

Finally, for moral support along the way I thank my wife Ceil, my father and my mother (who typed the paper), and my friend Professor Morton Loewenthal.